

## Searching for universal behaviour in superheated droplet detector with effective recoil nuclei

MALA DAS\* and SUSNATA SETH

Astroparticle Physics and Cosmology Division, Saha Institute of Nuclear Physics,  
1/AF Bidhan Nagar, Kolkata 700 064, India

\*Corresponding author. E-mail: mala.das@saha.ac.in

MS received 31 August 2012; revised 29 January 2013; accepted 31 January 2013

**Abstract.** Energy calibration of superheated droplet detector is discussed in terms of the effective recoil nucleus threshold energy and the reduced superheat. This provides a universal energy calibration curve valid for different liquids used in this type of detector. Two widely used liquids, R114 and C<sub>4</sub>F<sub>10</sub>, one for neutron detection and the other for weakly interacting massive particles (WIMPs) dark matter search experiment, have been compared. Liquid having recoil nuclei with larger values of linear energy transfer (LET) provides better neutron- $\gamma$  discrimination. Gamma ( $\gamma$ ) response of C<sub>4</sub>F<sub>10</sub> has also been studied and the results are discussed. Behaviour of nucleation parameter with the effective recoil nucleus threshold energy and the reduced superheat have been explored.

**Keywords.** Recoil; energy; calibration; superheat; neutron; weakly interacting massive particles.

**PACS Nos** 29.40.-n; 29.90.+r; 34.50.Bw; 95.35.+d

### 1. Introduction

Superheated droplet detector is used for both neutron detection and cold dark matter WIMPs (weakly interacting massive particles) search experiments under different operating temperatures and pressures [1–5]. Since its development in 1979, it has been mainly used in neutron dosimetry [6,7]. The detector consists of droplets of superheated liquids of low boiling points, suspended in viscous aquasonic gel or in polymer medium [1,2]. For neutron detection, the detector liquid normally used are: R12 (CCl<sub>2</sub>F<sub>2</sub>: b.p. –29.8°C), R114 (C<sub>2</sub>Cl<sub>2</sub>F<sub>4</sub>: b.p. 3.7°C), R134a (C<sub>2</sub>H<sub>2</sub>F<sub>4</sub>: b.p. –26°C) etc. High-energy X-ray radiotherapy machines are known to generate neutrons by photodisintegration or electron disintegration of atomic nuclei in various components of the accelerator, from various parts of the patient treatment room and also from the patient's body [8]. Superheated drop neutron dosimeter is a promising dosimeter for measuring neutron dose equivalent of complex energy, in and around the radiotherapy beam and in patients in the presence of large background of photon flux (three to four orders of magnitude larger than neutrons)

[9]. Extensive studies have been made with R114 as the sensitive liquid for the response of neutrons and  $\gamma$ -rays of this type of detector [10–12].  $C_2ClF_5$ ,  $CF_3I$ ,  $C_4F_{10}$  etc. are liquids used for dark matter search experiments [3–5]. WIMP-induced nuclear recoils are similar to neutron-induced nuclear recoils and therefore have several identical techniques for detection. By varying the operating condition, using liquids of different boiling points and compositions, and employing different pulse analysis techniques, neutrons,  $\alpha$ -particles,  $\gamma$ -rays etc., the unwanted backgrounds for cold dark matter search experiment can be identified.  $C_4F_{10}$  is the most favoured sensitive liquid for cold dark matter search experiment for PICASSO (project in Canada to search for supersymmetric objects) Collaboration [13,14]. In order to lower the threshold energy of the WIMPs-induced nuclear recoils to be detected, the  $\gamma$ -ray sensitive regions need to be investigated and developing efficient discrimination techniques is important for such dark matter experiments. In the present work, we perform a comparative study between two liquids, R114 and  $C_4F_{10}$ , with respect to neutron detection in a mixed neutron- $\gamma$  radiation field.

In the present work, the detector was fabricated in viscous aquasonic gel medium with  $C_4F_{10}$  as the sensitive liquid. In our earlier publication [12], the discrimination of neutron-induced events and  $\gamma$ -induced events for R114 detector has been described. In this work, we would like to study similar effects in  $C_4F_{10}$  detector and compare it with the observations of R114. In order to explore the neutron response, the  $\gamma$  response of  $C_4F_{10}$  detector has been studied. The energy released during the bubble nucleation process for  $\gamma$ -induced events is found to be independent of the operating temperature which provides important information on the  $\gamma$  background rejection technique. An attempt has been made successfully to determine a universal energy calibration curve with the ‘effective recoil nucleus threshold energy’ and the ‘reduced superheat’ [10] valid for different types of superheated liquids. One of the important parameters in bubble nucleation for this type of detector is the nucleation parameter [15]. It is reported that the nucleation parameter shows single line behaviour for  $C_4F_{10}$  liquid with operating temperature [16]. In the present work, studies on nucleation parameter obtained from different experiments have also been carried out to search for universal behaviour valid for both the liquids. This paper consists of a detailed description of the experiment performed, results obtained from the experiment and discussions of the physics importance of the results, followed by a conclusion section.

## 2. Present work

Superheated droplets of R114 and  $C_4F_{10}$  have been fabricated using aquasonic gel and glycerol as the supporting medium. The droplets were produced by adding refrigerant liquid on top of the degassed aquasonic gel in a stainless steel high pressure chamber and by stirring the liquid by a stirrer rotated with variable speed motor. The fabrication procedure is similar to the procedure described by Roy *et al* [17].

The response of  $C_4F_{10}$  detector in the presence of  $^{137}Cs$  (32.5 mCi)  $\gamma$ -source was measured by varying the temperature of the detector in the range of 30–60°C at the ambient pressure of 1 atm. The measurement has been done at various temperatures to find out  $\gamma$ -sensitive temperature for  $C_4F_{10}$ . Once the  $\gamma$ -sensitive temperature is identified, the measurement was done for neutrons below the  $\gamma$ -sensitive temperature. In this way, the measurement for neutrons becomes free from the  $\gamma$ -induced events. The  $\gamma$  response of the

R114 detector has already been studied for which the fabrication process was identical to that of  $C_4F_{10}$  in the present case [11,12]. The volume of both kinds of detectors was 40 ml in a glass vial with aquasonic gel as the supporting matrix of the superheated droplets. The detector was placed inside the water bath and the temperature of the bath was controlled by a temperature controller (Metravi, DTC-200) having a precision of  $\pm 1^\circ C$ . The acoustic pulse formed due to bubble nucleation was measured by a condenser microphone with a frequency response expanding up to about 30 kHz and the traces of the electrical pulse output was recorded in digital storage oscilloscope (Agilent Technologies, MSO7032A; 350MHz, 2 GSa/s). The commercially available condenser microphone contains two parallel plates of which one is made of a very light material which acts as a diaphragm. The diaphragm vibrates when struck by sound waves that change the distance between the two plates and as a result, its capacitance. This gives a corresponding electric signal and the intensity of the electric signal depends on the intensity of the acoustic signal falling on it. The development of the electronic circuit with the condenser microphone is described in [18]. The low-frequency signal is associated with the final stage of bubble nucleation. After the complete phase transition of a droplet, a freely oscillating vapour bubble is formed which oscillates around its equilibrium radius and the ambient equilibrium pressure with a resonant frequency (e.g. 6 kHz for  $C_4F_{10}$ ) that depends on the density of the surrounding medium [16].

For neutrons, the recoil nuclei are produced by the interaction of neutrons with the detector liquid, and these recoil nuclei deposit their energy in the liquid according to their linear energy transfer (LET) in the medium. The energy deposition in the sensitive liquid was calculated using SRIM code [19] for the carbon, fluorine ions in  $C_4F_{10}$  and carbon, chlorine, fluorine ions in R114 for neutron of 6 MeV maximum energy. The relation between the energy of the neutron and the operating temperature of the liquid can be obtained from the expression given below [11]:

$$\frac{W}{kr_c}(T, P) = \frac{dE}{dx}(E_n), \quad (1)$$

where  $W$  is the critical energy for bubble formation obtained from reversible thermodynamics [20],  $r_c$  is the critical bubble radius and  $k$  is the nucleation parameter which has been found to be equal to 0.11 for neutron-induced nucleation upto around 10 MeV for R114 liquid [11]. For  $C_4F_{10}$ ,  $k$  has been calculated at  $25^\circ C$  using the above expression and found to be equal to 0.15. In the calculation, the threshold neutron energy was taken as 371 keV at  $25^\circ C$  from experiment [21].

The present experiment was performed with both R114 and  $C_4F_{10}$  in the presence of  $^{252}Cf$  (3.2  $\mu Ci$ ) fission neutron source at the neutron-sensitive temperatures,  $55^\circ C$  for R114 and  $35^\circ C$  for  $C_4F_{10}$ . The experiment has also been done at both the neutron- and  $\gamma$ -sensitive temperatures,  $70^\circ C$  for R114 [11] and  $55^\circ C$  for  $C_4F_{10}$ .

Trace of each pulse is recorded in digitized storage oscilloscope and the power ( $P$ ) is calculated from the amplitudes of the pulses. The power  $P$  which is a measure of the energy released during the bubble nucleation process, is defined as  $\log_{10}(\sum_i |V_i|^2)$  where  $V_i$  is the pulse amplitude (in volt) of the digitized acoustic pulse at the  $i$ th time bin, and the summation extends over the duration of the signal [12].

For constructing the universal energy calibration curve, the 'effective recoil nucleus' has been determined for different liquids from the available experimental results. It is

known that the effective recoil nucleus is different for different liquids and it also depends on the energy region of interest [22]. The recoil nucleus having the maximum  $dE/dx$  at a given energy is considered as the effective recoil nucleus. The results from the neutron calibration at different temperatures for different liquids,  $C_4F_{10}$ ,  $C_4F_8$  (b.p.  $-9.1^\circ C$ ), R114, R142B ( $C_2H_3ClF_2$ : b.p.  $-6.9^\circ C$ ) are obtained from different experiments reported in [10,11,15,21,23]. The recoil nuclei receive the maximum energy from the incident neutron through the elastic head-on collision and that energy is considered in calculating the effective recoil nucleus threshold energy. The ‘effective recoil nucleus threshold energy’ is then plotted for the liquids  $C_4F_{10}$ ,  $C_4F_8$ , R114, R142B with the ‘reduced superheat  $s$ ’. The reduced superheat  $s$  is expressed as,  $s = (T - T_b)/(T_c - T_b)$  [10] where  $T_b$  is the boiling point,  $T_c$  is the critical temperature and  $T$  is the ambient temperature of the liquid.

Attempt has also been made to search for the single line behaviour of the ‘nucleation parameter’ for the two liquids,  $C_4F_{10}$  and R114. There are different ways of expressing the nucleation parameter, the details of which can be found in ref. [15]. The nucleation parameters  $a$  and  $k$  are defined as

$$E_c = ar_c \left( \frac{dE}{dx} \right)_{L_{\text{eff}}},$$

where

$$E_c = \frac{4\pi}{3}r_c^3 H + 4\pi r_c^2 \left[ \gamma(T) - T \frac{d\gamma}{dT} \right] + \frac{4\pi}{3}r_c^3 P_0$$

and

$$W = kr_c \left( \frac{dE}{dx} \right)_{L_{\text{eff}}},$$

where

$$W = \frac{16\pi\gamma^3(T)}{3[P_v(T) - P_0]^2}.$$

Here  $E_c$  is the critical energy required for bubble formation,  $H$  is the evaporation heat per unit liquid volume,  $r_c$  is the critical radius of the vapour bubble,  $\gamma(T)$  is the surface tension at the temperature  $T$ ,  $P_v(T)$  is the vapour pressure of the liquid,  $P_0$  is the ambient liquid pressure and  $L_{\text{eff}}$  is the effective path length along the track of the particle [15]. The energy deposition over the length  $L_{\text{eff}}$  plays a significant role in bubble nucleation. Available results on nucleation parameters from different experiments have been expressed in terms of the parameter  $a$  and also calculated from eq. (1), by converting  $k$  to  $a$  using the following expression [15]:

$$a = k \frac{E_c}{W}. \tag{2}$$

### 3. Results and discussions

The result of the measurements with  $^{137}\text{Cs}$   $\gamma$ -source as a function of temperature is shown in figure 1. In the present experiment, the threshold temperature for  $\gamma$  sensitivity of the

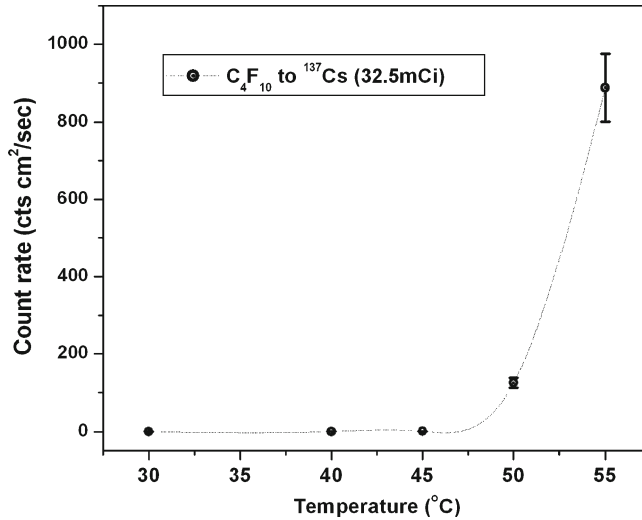


**Figure 1.** Observed response of  $C_4F_{10}$  detector as a function of temperature in the presence of  $^{137}Cs$   $\gamma$ -source.

unpurified detector fabricated in normal (non-clean room) condition is found to be in the range of  $45^\circ C < T_{th} \leq 50^\circ C$ . Therefore, for studying the neutron sensitivity in the present work, we restricted the temperatures to be well below  $45^\circ C$  in the  $\gamma$ -insensitive region. We noted in this connection that the  $\gamma$ -sensitive threshold temperature of purified  $C_4F_{10}$  detector, fabricated in clean room environment and irradiated with  $^{22}Na$  ( $0.7 \mu Ci$ ), as reported by PICASSO experiment was above  $55^\circ C$  [13,14]. Differential power ( $P$ )

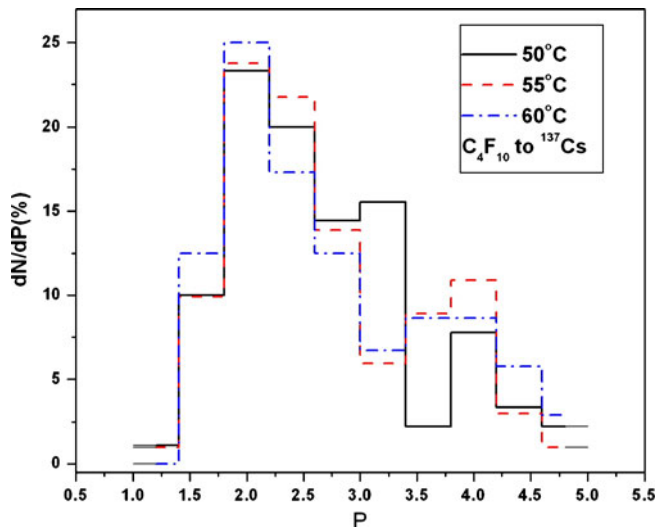


**Figure 2.** Observed differential power distribution of pulses of  $C_4F_{10}$  detector in the presence of  $^{137}Cs$   $\gamma$ -source.

distribution [12] of the pulses obtained at different temperatures for  $^{137}\text{Cs}$   $\gamma$ -ray-induced events in  $\text{C}_4\text{F}_{10}$  is shown in figure 2. It is reported that the peak of the distribution of the integrated signal power,  $P_{\text{var}}$ , for neutron-induced events for  $\text{C}_4\text{F}_{10}$  detector depends on the temperature [13]. The measured temperature dependence of the peaks serves to define temperature-dependent cut on  $P_{\text{var}}$  in order to reject the non-particle-induced events [13,14]. Figure 2 shows that the peak of the power distribution for  $\gamma$ -induced events is independent of the operating temperature. The present result shows that a temperature-independent cut on the power distribution can be used to reject  $\gamma$ -induced events for superheated droplet detector employing  $\text{C}_4\text{F}_{10}$  as sensitive liquid in soft aquasonic gel supporting medium, for neutron detection in mixed neutron- $\gamma$  radiation field and also for WIMPs search experiment.

The calculated values of the critical radius and the critical energy for bubble formation at  $25^\circ\text{C}$  for both the liquids are shown in table 1. It is observed from table 1 that the critical energy for bubble formation is less for  $\text{C}_4\text{F}_{10}$  than for R114. Therefore, it is expected that the incident neutron energy needed to trigger the nucleation would be less for  $\text{C}_4\text{F}_{10}$  than for R114, which is also observed in experiments [10,11,15,21], as shown in figure 3. For lower energy neutron detection,  $\text{C}_4\text{F}_{10}$  would be the good candidate as sensitive liquid in superheated droplet detector. The solid line in figure 3 is obtained by employing eq. (1) and the experimental points are obtained from different monoenergetic neutron experiments with  $\text{C}_4\text{F}_{10}$  and R114 by different workers [10,11,15,21].

The  $dE/dx$  curves of different constituent nuclei in R114 and  $\text{C}_4\text{F}_{10}$  are shown in figure 4. The two horizontal lines (dashed and dashed-dotted) in figure 4 are the critical LETs for bubble nucleation in R114 at  $55^\circ\text{C}$  and in  $\text{C}_4\text{F}_{10}$  at  $35^\circ\text{C}$ , calculated using eq. (1). Figure 4 shows that  $dE/dx$  of chlorine is much higher in the lower energy region than  $dE/dx$  of carbon (C) and fluorine (F) in both the liquids. Since the peak energy of neutrons from  $^{252}\text{Cf}$  fission neutron source occurs at about 700 keV [18], the maximum energies of recoil nuclei obtained from elastic head-on collision with neutron are 74.6 keV, 198.8 keV, 133.0 keV for chlorine, carbon and fluorine respectively. At these low recoil energy regions, because of the high LET of chlorine, energy deposited within the effective length required for bubble nucleation at a given temperature is larger in R114 than those due to carbon and fluorine in  $\text{C}_4\text{F}_{10}$ . Therefore, the discrimination of events

**Table 1.** Physical and calculated parameters for  $\text{C}_4\text{F}_{10}$  and R114.

Liquids	Density (1.013 bar at b.p.) (g/cc)	Critical radius at $25^\circ\text{C}$ ( $r_c$ ) ( $\mu\text{m}$ ) (Calculated)	Critical energy at $25^\circ\text{C}$ ( $W$ ) (keV) (Calculated)	Critical temperature ( $^\circ\text{C}$ )	Critical pressure (bar)
$\text{C}_4\text{F}_{10}$ (b.p. $-1.7^\circ\text{C}$ )	1.594	0.133	4.91	113.0	24.27
R114 ( $\text{C}_2\text{Cl}_2\text{F}_4$ : b.p. $3.7^\circ\text{C}$ )	1.527	0.194	10.81	145.7	32.63

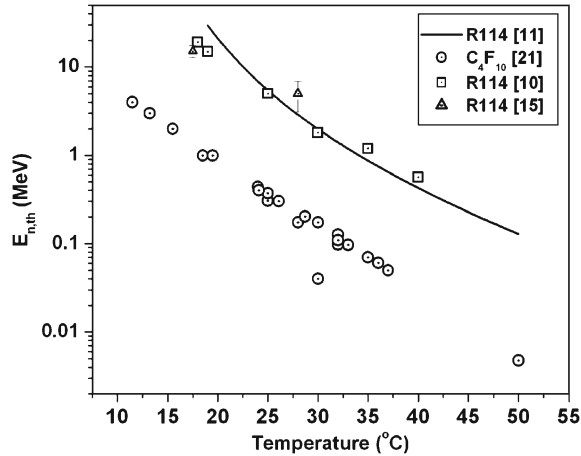


**Figure 3.** Variation of threshold neutron energy ( $E_{n,th}$ ) with temperature for  $C_4F_{10}$  and R114.

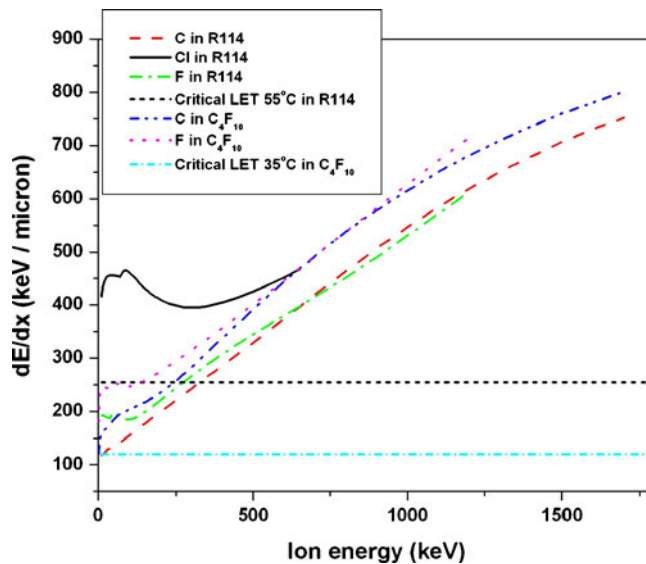


**Figure 4.** Variation of  $dE/dx$  for C, Cl, F in R114 and for C, F in  $C_4F_{10}$ .

caused by nuclear recoils and by the  $\gamma$ -rays are more prominent in R114 than in  $C_4F_{10}$ . In figure 5,  $C_4F_{10}$  at 35°C and R114 at 55°C are sensitive to neutrons from  $^{252}Cf$  source and  $C_4F_{10}$  at 55°C and R114 at 70°C become also sensitive to  $\gamma$ -rays from  $^{252}Cf$  source. Figure 5 shows that for R114, neutron- and  $\gamma$ -induced events are well separated, while for  $C_4F_{10}$  it is not. It is also clear from figure 5 that the P-distribution for  $\gamma$ -induced events for both the liquids,  $C_4F_{10}$  and R114, falls in the same region and it does not depend on the composition of the liquid.

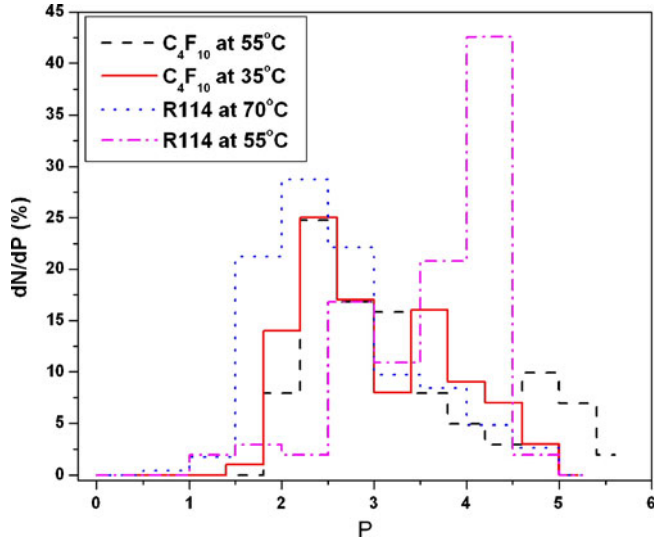


**Figure 5.** Observed differential power distributions at different temperatures for  $C_4F_{10}$  and R114 in the presence of  $^{252}Cf$  fission neutron source.

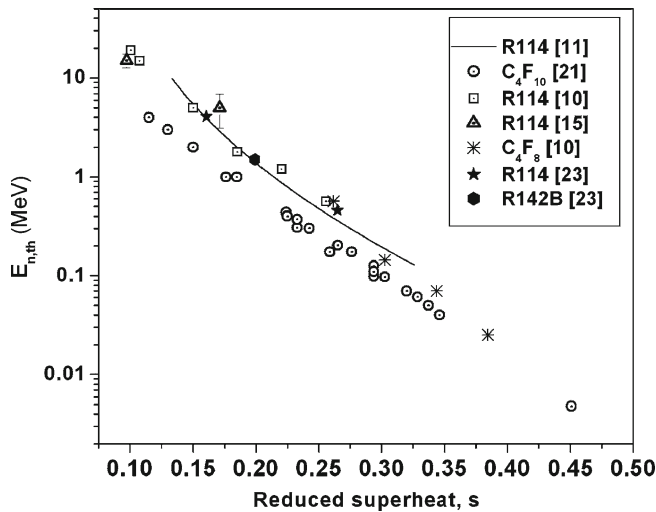


**Figure 6.** Variation of threshold neutron energy  $E_{n,th}$  as a function of reduced superheat  $s$  for different liquids.

In order to obtain a universal energy calibration curve, the data are plotted in figure 6, in terms of the ‘threshold neutron energy’ for the liquids R114,  $C_4F_{10}$ ,  $C_4F_8$ , R142B obtained from different experiments with the ‘reduced superheat’  $s$  [10,11,15,21,23]. Here the data for the different liquids do not follow a single line. In figure 7, we replot the data used in figure 6 in terms of the ‘effective recoil nucleus threshold energy’ with the ‘reduced superheat’  $s$ . In this case, it is observed that the experimental data for all the

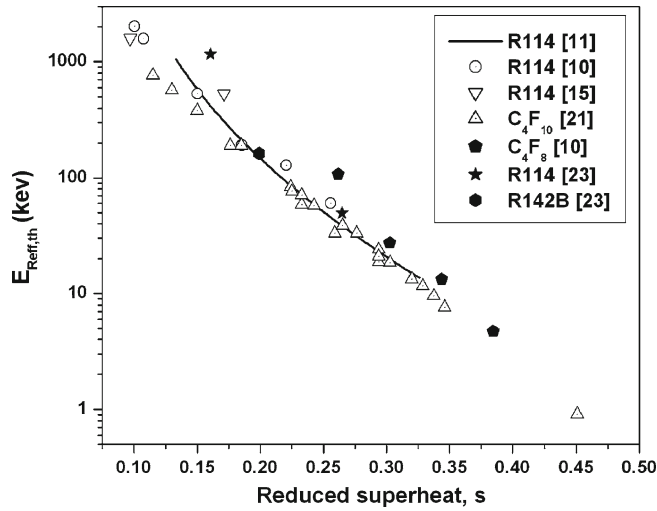


**Figure 7.** Variation of effective recoil nucleus threshold energy  $E_{\text{Reff,th}}$  as a function of reduced superheat  $s$ .

liquids fall on a single line. In the plot,  $\text{C}_4\text{F}_{10}$  data are obtained from ref. [21], R114 data from refs [10,11,15,23],  $\text{C}_4\text{F}_8$  data from ref. [10] and R142B data from ref. [23]. Experimental observation shows that about 90% of the critical temperature can be reached for the superheated liquid droplets [24]. Therefore, here we define  $s'$  by replacing  $T_c$  with

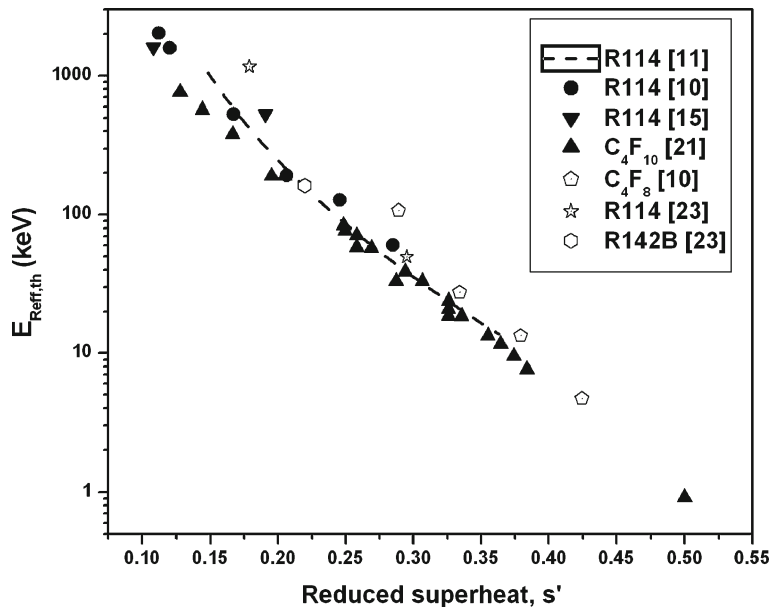


**Figure 8.** Variation of effective recoil nucleus threshold energy  $E_{\text{Reff,th}}$  as a function of reduced superheat  $s'$ .

$0.9T_c$  in the expression of  $s$  and another set of datapoints with  $s'$  is obtained which is shown in figure 8. In both the cases, either with  $s$  or with  $s'$ , the datapoints fall on the single curve. Thus, a plot of the ‘effective recoil nucleus threshold energy’ vs. the ‘reduced superheat’ ( $s$  or  $s'$ ) can provide a universal energy calibration curve for superheated droplet detector. The effective recoil nucleus is more fundamental in bubble nucleation

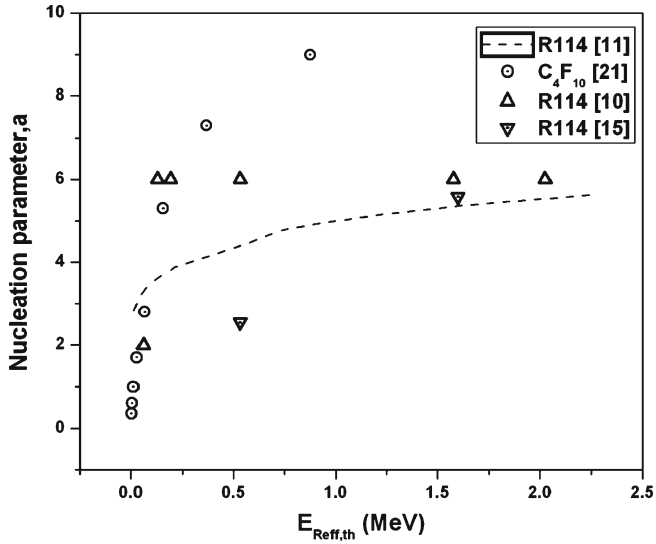


**Figure 9.** Nucleation parameter  $a$  as a function of effective recoil nucleus threshold energy  $E_{\text{Reff,th}}$ .

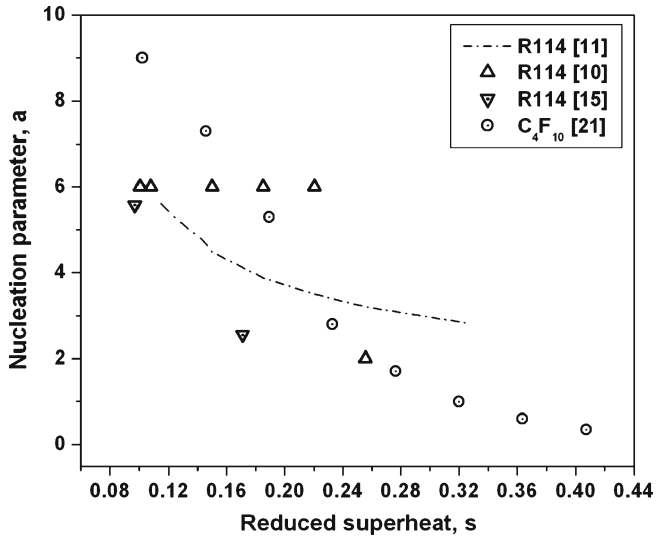


**Figure 10.** Nucleation parameter  $a$  as a function of reduced superheat  $s$ .

than in incident neutron. The effective recoil nuclei are the characteristics of the liquid. Therefore, universal behaviour is observed while plotting with effective recoil nuclei threshold energy but not with the threshold neutron energy.

Figures 9 and 10 show the variation of nucleation parameter for  $C_4F_{10}$  and R114 as a function of effective recoil nucleus threshold energy and the reduced superheat respectively. The solid line is obtained from eq. (1) and by converting  $k$  to  $a$  using eq. (2). The nucleation parameter varies significantly for  $C_4F_{10}$  in figures 9 and 10 but not as for R114. The possible explanation is as follows: the nucleation parameter depends on the energy deposition, temperature and pressure of the sensitive liquid. The energy deposition again depends on the mass of the recoil nuclei. Therefore, it depends on the composition of the sensitive liquids. For R114, the effective recoil nucleus is chlorine and for  $C_4F_{10}$ , it is fluorine, in the energy range of interest. Figure 4 shows that  $dE/dx$  of chlorine does not vary significantly as it is varied for fluorine in  $C_4F_{10}$ . Therefore, in figures 9 and 10, the results for different liquids do not appear to be on single line while plotted with the effective recoil nucleus threshold energy and the reduced superheat independently and appears to be dependent on both the energy of the particle and the type of the sensitive liquid.

#### 4. Conclusions

A comparative study is performed on the response of R114 and  $C_4F_{10}$  detector, in a mixed neutron- $\gamma$  radiation field. Neutron- $\gamma$  discrimination is observed to be more prominent in R114, the liquid having recoil nuclei with larger values of LET, than that of  $C_4F_{10}$ . Although the probability of  $\gamma$ -induced nucleation increases with increase in temperature in  $C_4F_{10}$  liquid droplets, the peak of the power distribution is observed to be independent of the operating temperature. Studies on the nucleation parameter for the two liquids do not provide a universal behaviour while plotted either with reduced superheat or with effective recoil nucleus threshold energy. The present study provides important information on the energy calibration of such a detector. The universal energy calibration curve for superheated droplet detector has been explored successfully utilizing the 'effective recoil nucleus threshold energy' and the 'reduced superheat' that can be utilized for both neutron detection and the WIMPs dark matter search experiments.

#### Acknowledgements

The authors sincerely acknowledge Prof. Viktor Zacek, University of Montreal, Canada and Prof. Pijushpani Bhattacharjee, Saha Institute of Nuclear Physics, Kolkata, India for encouragement and useful discussions. Authors are grateful to Prof. B K Chatterjee, Department of Physics, Bose Institute, Kolkata, India, for providing  $^{137}\text{Cs}$  gamma source.

#### References

- [1] R E Apfel, US Patent 4143274 (1979)
- [2] H Ing and H C Birnboim, *Nucl. Tracks Radiat. Meas.* **8**, 285 (1984)
- [3] PICASSO Collaboration: M Barnabe-Heider *et al*, *Nucl. Instrum. Methods A* **555**, 184 (2005)

- [4] T Morlat, M Felizardo, F Giuliani, T A Girard, G Waysand, R F Payne, H S Miley, A R Ramos, J G Marques, R C Martins and D Limagne, *Astropart. Phys.* **30**, 159 (2008)
- [5] W J Bolte, J I Collar, M Crisler, J Hall, D Holmgren, D Nakazawa, B Odom, K OSullivan, R Plunkett, E Ramberg, A Raskin, A Sonnenschein and J D Vieira, *Nucl. Instrum. Methods A* **577**, 569 (2007)
- [6] R E Apfel and S C Roy, *Nucl. Instrum. Methods A* **219**, 582 (1984)
- [7] R E Apfel and S C Roy, *Rad. Prot. Dosim.* **10**, 327 (1985)
- [8] S C Roy, *Rad. Phys. Chem.* **61**, 271 (2001)
- [9] S C Roy and G A Sandison, *Med. Phys.* **27**, 1800 (2000)
- [10] F D'Errico, *Nucl. Instrum. Methods B* **184**, 229 (2001)
- [11] Mala Das, B K Chatterjee, B Roy and S C Roy, *Rad. Phys. Chem.* **66**, 323 (2003)
- [12] Mala Das, S Seth, S Saha, S Bhattacharya and P Bhattacharjee, *Nucl. Instrum. Methods A* **622**, 196 (2010)
- [13] PICASSO Collaboration: F Aubin *et al*, *New J. Phys.* **10**, 103017 (2008)
- [14] PICASSO Collaboration: S Archambault *et al*, *Phys. Lett. B* **682**, 185 (2009)
- [15] Mala Das and Teroku Sawamura, *Nucl. Instrum. Methods A* **531**, 577 (2004)
- [16] PICASSO Collaboration: S Archambault *et al*, *New J. Phys.* **13**, 043006 (2011)
- [17] B Roy, B K Chatterjee and S C Roy, *Radiat. Meas.* **29**, 173 (1998)
- [18] Mala Das, A S Arya, C Marick, D Kanjilal and S Saha, *Rev. Sci. Instrum.* **79(11)**, 113301 (2008)
- [19] J F Ziegler, M D Ziegler and J P Biersack, *Stopping and Range of Ions in Matter 2008 (SRIM.com)*
- [20] J W Gibbs, *Ransl. Conn. Acad.* **III**, 108 (1875)
- [21] PICASSO University of Montreal group (2010), personal communications
- [22] R E Apfel, Y C Lo and S C Roy, *Phys. Rev. A* **31**, 3194 (1985)
- [23] S C Roy, R E Apfel and Y C Lo, *Nucl. Instrum. Methods A* **255**, 199 (1987)
- [24] Mala Das, B K Chatterjee, B Roy and S C Roy, *Phys. Rev. E* **62**, 5843 (2000)